Dust and sea surface temperature forcing of the 1930's 'Dust Bowl' drought.

Manuscript submitted to Geophysical Research Letters
January 31, 2008

Benjamin I. Cook (corresponding author)
Lamont-Doherty Earth Observatory
Ocean and Climate Physics
61 Route 9W
PO Box 1000
Palisades, NY 10964-8000
bc9z@ldeo.columbia.edu
Ph: 434-409-9233

NASA Goddard Institute for Space Studies
2880 Broadway
New York, NY 10025

Ron L. Miller
NASA Goddard Institute for Space Studies
2880 Broadway
New York, NY 10025

Richard Seager
Lamont-Doherty Earth Observatory
Ocean and Climate Physics
61 Route 9W
PO Box 1000
Palisades, NY 10964-8000

Abstract.

Droughts over the central United States (US) are modulated by sea surface temperature (SST) variations in the eastern tropical Pacific. Many models, however, are unable to reproduce the severity and spatial pattern of the 'Dust Bowl' drought of the 1930s with SST forcing alone. We force an atmosphere general circulation model with 1930s SSTs and model-generated dust emission from the Great Plains region. The SSTs alone force a drought over the US similar to observations, but with a weaker precipitation anomaly that is centered too far south. Inclusion of dust radiative forcing, centered over the area of observed wind erosion, increases the intensity of the drought and shifts its center northward. While our conclusions are tempered by limited quantitative observations of the dust aerosol load and soil erosion during this period, our study suggests that unprecedented atmospheric dust loading over the continental US exacerbated the 'Dust Bowl' drought.

Keywords: drought, dust, land surface feedbacks, Dust Bowl, aerosols

65 **Introduction.**

66 Droughts in the midlatitudes of both hemispheres are often associated with sea surface
67 temperature (SST) anomalies in the eastern tropical Pacific, specifically the La Nina
68 phase of the El Nino Southern Oscillation (Seager et al, 2005a). Examples over North
69 America include droughts during the 1950s and latter part of the 19th century (Herweijer
70 et al, 2006; Seager et al 2005b), as well as the most recent and ongoing drought in the
71 western US (Hoerling and Kumar, 2003; Seager, 2007). Modeling evidence suggests
72 SST forcing was at least partially responsible for the drought during the 1930s known as
73 the 'Dust Bowl' (Schubert et al, 2004a,b; Seager et al, 2005b, 2007). Models, however,
74 have difficulty reproducing the severity and spatial pattern of the Dust Bowl drought,
75 instead producing droughts that, while superficially similar to observations, are too weak
76 and centered in the southwest rather than the central and northern Great Plains as
77 observed (e.g., Schubert et al, 2004a,b, Seager et al, 2005b, 2007). Seager et al. (2007)
78 used millennium long tree ring records to argue that the spatial pattern of the Dust Bowl
79 drought was unique in the era of instrumental observations. This has led to speculation
80 that the drought may have been amplified by land surface feedbacks related to the large-
81 scale land degradation over the Great Plains region during this decade. A consequence of
82 this degradation was massive wind erosion and dust storms on an unprecedented scale
83 (Chepil, 1957; Seager et al, 2007; Worster, 1979).

84 Dust storms were widespread throughout the United States during the 1930s (e.g.,
85 Mattice, 1935a,b). High wind erosion resulted from a variety of convergent factors,
86 including low soil moisture from the drought, poor land use practices, and the
87 replacement of drought resistant native grasslands with drought susceptible wheat crops

88 (Hansen and Libecap, 2004). Recent studies have shown the potential for high dust
89 loading in the atmosphere to suppress precipitation (e.g., Miller and Tegen, 1998;
90 Rosenfeld, 2001). Dust effectively scatters and absorbs shortwave radiation while
91 absorbing and emitting longwave radiation. By reducing the net radiation into the surface
92 beneath the aerosol layer, dust reduces evaporation and thus precipitation (Miller and
93 Tegen, 1998). There is thus a strong potential for dust forcing to exacerbate drought
94 during the Dust Bowl. Here we investigate the contribution of SST and dust radiative
95 forcing to the 1930s Dust Bowl drought, using a state of the art atmosphere general
96 circulation model coupled to a dust emission and transport model. We consider the
97 effects of SST forcing alone, and the influence of SST in combination with dust radiative
98 forcing.
99
100 **Models.**
101 The Goddard Institute for Space Studies (GISS) ModelE is a state of the art atmospheric
102 general circulation model, incorporating significant updates to the physics compared to
103 previous versions, and capable of calculating the evolution of several aerosol and
104 chemical tracers as a function of the model climate (Schmidt et al, 2006; Shindell et al,
105 2007). Simulations of modern day climate in ModelE compare favorably with
106 observations, with some notable biases, particularly in the subtropical marine
107 stratocumulus regions. ModelE is unusually successful at simulating the observed annual
108 cycle of precipitation over the Great Plains and Mexico, along with interannual variations
109 in precipitation during the second half of the 20th century (Ruiz-Barradas and Nigam,
110 2006). We use a version of ModelE coupled to a model of mineral dust aerosols (Miller

et al, 2006). Given 'natural' dust sources (i.e., excluding sources created by anthropgenic land degradation: Ginoux et al, 2001) and forced by present day ModelE climate, the dust model reproduces (within the range of observational uncertainty) the seasonal atmospheric dust cycle, as well as the magnitude and pattern of atmospheric dust loading (Cakmur et al, 2006; Miller et al, 2006). Dust within the model interacts with radiation in ModelE (absorbing, emitting, and reflecting longwave and shortwave), but does not impact cloud microphysics.

Experimental Setup.

We conduct three sets of experiments comprised of five member ensemble model runs, with each member of the ensemble starting from a different initial condition. As a control experiment, ModelE is run with observed SSTs for the period 1920-1929 and without dust (Experiment 1). To examine SST forcing of the Dust Bowl drought, we then force the model with observed SSTs for 1932-1939, again without dust (Experiment 2). For our final experiment, we examine the combined impact of SST and dust forcing on the Dust Bowl drought by forcing the model with SSTs for 1932-1939 and active dust emission over the Great Plains (Experiment 3). Dust sources within the model are defined according to Ginoux et al (2001), and correspond to topographic lows with bare ground, areas likely to accumulate sediment over geologic timescales (i.e., natural sources). This definition excludes additional dust sources created by anthropogenic disturbance. To simulate wind erosion and atmospheric dust loading during the Dust Bowl, we add a dust source over the Great Plains, over the approximate region of significant wind erosion (Figure 2; 34°N-48°N, 102.5°W-92.5°W; Hansen and Libecap,

2004). Emission as a function of wind speed is scaled so that the dust cycle from natural sources generally agrees with a worldwide array of observations (Cakmur et al. 2006). However, sources created by land degradation are expected to be initially more vulnerable to wind erosion, resulting in greater emission compared to natural sources (e.g. Tegen et al 1996, Mahowald et al. 2002, Yoshioka et al 2005). We specify the disturbed sources over the Great Plains to be three times more productive compared to natural sources for a given wind event. While the precise expansion and productivity of dust sources due to land degradation is not known, we try to constrain this below by comparing the additional dust emission by agricultural sources to estimates of observed soil loss during the Dust Bowl.

Results and Discussion.

Figure 1 shows dust emission from the land surface, dust deposition to the surface, and net dust emission (emission minus deposition) from our Experiment 3 (SST+Dust) for 1932-1939, for the region of the imposed anthropogenic dust source. Figure 2 outlines the area of the new dust source and the additional atmospheric dust loading in Experiment 3 (SST+Dust minus SST Only). Quantifying observations of both dust emission and atmospheric dust loading during the 1930s is difficult. While there is much anecdotal and qualitative evidence for high dust emission and atmospheric concentrations, few hard numbers are available. One estimate for 1935 alone puts the loss of topsoil to wind erosion at roughly 771 million metric tons (Hansen and Libecap, 2004; Johnson, 1947). Net dust emission from the model for 1935 is of the same order of magnitude, but only about half of the 771 million metric tons needed to match

observations. A comparison between atmospheric dust loading from this experiment (Figure 2) and more qualitative dust storm maps from the period (not shown; Mattice, 1935b) suggests that the spatial pattern of atmospheric loading is reasonable. For the moment, we note that the productivity of disturbed sources compared to natural ones is a fundamental uncertainty that can be resolved only with more definitive observations of the aerosol load and soil erosion during the Dust Bowl.

We focus on spring and summer precipitation anomalies (March through August). Figure 3 shows box and whisker plots of precipitation anomalies from the GHCN precipitation dataset (Vose et al, 1992) and our model experiments, averaged over the central US, the center of action for the Dust Bowl drought (30ºN-48ºN, 105ºW-85ºW). All anomalies (for the model and GHCN data) are relative to the 1920-1929 average, a period of fairly wet conditions over the US. The model, forced with 1932-1939 SSTs alone, produces a drying as seen in the GHCN data, with a reduced magnitude. Nonetheless, ~71% of the total of 40 simulated years within the 5 ensemble members were drier than the ensemble mean for the 1920s simulation. When dust forcing is included with the SST forcing, the drought intensifies, as seen in the overall shift of the distribution towards negative precipitation anomalies. The spatial pattern and intensity of the drought also changes with the inclusion of dust (Figure 4). SST forcing alone leads to fairly muted precipitation anomalies in the central plains; the resulting pattern is not dry enough and the drought extends much too far south into northern Mexico. With SST+Dust forcing, the drought intensifies and the center of drying moves north and east. Several notable differences between model and observations remain. In the model, the center of drought is shifted too far to the northeast, leading to a Great Lakes region that is

too dry. The drought also does not extend far enough north, into the central Canadian plains. Parts of Mexico still show a dry anomaly, contrary to the GHCN dataset that actually shows a wet anomaly over much of Mexico. As with other studies, our model is unable to reproduce the large warming during the drought (not shown). It remains unclear how much of the discrepancy with observations results from uncertainty in the dust sources, compared to factors not considered here. In our experiments, the mechanisms for precipitation reductions associated with increased dust loading are consistent with other studies where reduced net radiation into the surface beneath the dust layer reduces evaporation and precipitation (e.g., Miller and Tegen, 1998; Yoshioko et al, 2007). We subtract (using the ensemble mean results) SST forcing from the SST+Dust forcing experiments to examine the added effect of dust. Increased atmospheric dust loading in the SST+Dust case (Figure 2) leads to reductions in net surface radiation (Supplemental Figure 1), centered under the region of highest atmospheric dust loading. Reductions in surface radiation drive reductions in surface evaporation and latent heating (Supplemental Figure 2), leading to a negative precipitation feedback. Evaporative and soil moisture feedbacks during the Dust Bowl drought are supported by a previous study (Schubert et al, 2004)

Conclusions.

Within GISS ModelE, SST forcing alone reproduces the drought during the 1930s, but one that is too weak and centered too far to the south. By adding in a dust source over the main region of dust emission during this period, the model generates a more intense drought that has a modestly more realistic spatial pattern. For this study we also did not

consider other potential feedbacks (e.g., vegetation) that may have influenced the drought. These results support the notion that wind erosion and atmospheric dust concentrations that were unprecedented in the historical record could have acted as a positive feedback to drought during the Dust Bowl and potentially contributed to it being centered further to the north than typical tropical SST-forced droughts (Seager et al. 2007). Results here are preliminary, and serve largely as a starting point for future work. The dust emission, for example, should be much better constrained and other choices for source productivity have been made (e.g. Koven, 2006). Indeed the balance of evidence suggests that the modeled dust emission is smaller than what actually occurred and, hence, the results presented here may underestimate the impacts of Dust Bowl wind erosion. Thus, our study identifies the quantitative calculation of net soil loss and the pattern of the aerosol burden resulting from disturbed sources as key prerequisites for understanding the singular magnitude of the Dust Bowl.

Acknowledgments

We thank Tom Gill, Greg Okin, and Jan Perlwitz for helpful discussions. This work is supported by the NOAA Global Change Postdoctoral Program (BIC) and the Climate Dynamcis Program of the National Science Foundation through ATM-06-20066. RLM also received support from the NASA Atmospheric Composition Program and RS was supported by NOAA grants NA06OAR4310151 and NA03OAR4320179. This paper is LDEO contribution #0000.

References:

Cakmur, R.V., R.L. Miller, Ja. Perlwitz, I.V. Geogdzhayev, P. Ginoux, D. Koch, K.E. Kohfeld, I. Tegen, and C.S. Zender, 2006: Constraining the global dust emission and load by minimizing the difference between the model and observations. *J. Geophys. Res.*, **111**, D06207, doi:10.1029/2005JD005791.

Chepil WS (1957): Dust Bowl: Causes and effects. *Journal of Soil and Water Conservation*, **12**, 108-111

Cook, E.R., C. Woodhouse, C. M. Eakin, D. M. meko and D. W. Stahle (2004): Long term aridity changes in the western United States. *Science,* 306, 1015-1018.

Ginoux P, M Chin, I Tegen, JM Prospero, B Holben, O Dubovik, SJ Lin (2001): Sources and distributions of dust aerosols simulated with the GOCART model. *Journal of Geophysical Research*, **106**, 20,255-20,273

Hansen ZK, GD Libecap (2004): Small Farms, Externalities, and the Dust Bowl of the 1930s. *Journal of Political Economy*, **112**, 665-694

Herweijer C, R Seager, ER Cook (2006): North American droughts of the mid to lates Nineteenth Century: History, simulation, and implications for Medieval drought. *The Holocene*, **16**, 159-171

249 Hoerling MP, A Kumar (2003): The Perfect Ocean for Drought. *Science*, **299**, 691-694.
250
251 Johnson V (1947): *Heaven's Tableland: The Dust Bowl Story*. New York: Farrar, Straus
252
253 Koven CD (2006): *Ph.D. Dissertation, entitled "On the sources, composition, and*
254 *climatic effects of mineral dust in the atmosphere"*, University of California, Berkeley
255
256 Mahowald, N. M., C. S. Zender, C. Luo, D. Savoie, O. Torres, and J. del Corral,
257 Understanding the 30-year Barbados desert dust record, J. Geophys. Res., 107(D21),
258 4561, doi:10.1029/2002JD002097, 2002
259
260 Mattice WA (1935a): Dust Storms, November 1933 to May 1934. *Monthly Weather*
261 *Review*, **63**. 53-55
262
263 Mattice WA (1935b): Dust Storms. *Monthly Weather Review*, **63**, 113-115
264
265 Miller RL, I Tegen (1998): Climate Response to Soil Dust Aerosols. *Journal of Climate*,
266 **11**, 3247-3267
267
268 Miller RL, RV Cakmur, J Perlwitz, IV Geogdzhayev, P Ginoux, D Koch, KE Kohfeld, C
269 Prigent, R Ruedy, GA Schmidt, I Tegen (2006): Mineral dust aerosols in the NASA
270 Goddard Institute for Space Studies ModelE atmospheric general circulation model.
271 *Journal of Geophysical Research*, doi:10.1029/2005JD005796

Rosenfeld D, Y Rudich, R Lahav (2001): Desert dust suppressing precipitation: A possible desertification feedback loop. *Proceedings of the National Academy of Sciences*, **98**, 5975-5980

Ruiz-Barrada A and S Nigam (2006): IPCC's Twentieth-Century Climate Simulations: Varied Representations of North American Hydroclimate. *Journal of Climate*, **19**, 4041-4058

Schmidt GA, R Ruedy, JE Hansen, I Aleinov, N Bell, M Bauer, S Bauer, B Cairns, V Canuto, Y Cheng, AD Genio, G Faluvegi, AD Friend, TM Hall, Y Hu, M Kelley, NY Kiang, D Koch, AA Lacis, J Lerner, KK Lo, RL Miller, L Nazerenko, V Oinas, J Perlwitz, J Perlwitz, D Rind, A Romanou, GL Russell, M Sato, DT Shindell, PH Stone, S Sun, N Tausnev, D Thresher, MS Yao (2006): Present-Dat Atmospheric Simulation Using GISS ModelE: Comparison to In Situ, Satellite, and Reanalysis Data. *Journal of Climate*, **19**, 153-192.

Schubert SD, MJ Suarez, PJ Region, RD Koster, JT Bacmeister (2004a): On the Cause of the 1930s Dust Bowl. *Science*, **303**, 1855-1859

Schubert SD, MJ Suarez, PJ Region, RD Koster, JT Bacmeister (2004b): Causes of long-term drought in the United States Great Plains. *J. Climate*, 17, 485-503.

Seager R, N Harnik, WA Robinson, Y Kushnir, M Ting, HP Huang, J Velez (2005a): Mechanisms of ENSO-forcing of hemispherically symmetric precipitation variability. *Quarterly Journal of the Royal Meteorological Society*, **131**, 1501-1527

Seager R, Y Kushnir, C Herweijer, N Naik, J Velez (2005b): Modeling of tropical forcing of persistent droughts and pluvials over western North America: 1856-2000. *Journal of Climate*, **18**, 4068-4091

Seager R (2007): The Turn of the Century North American Drought: Global Context, Dynamics, and Past Analogs. *Journal of Climate*, **20**, 5527-5552

Seager R, Y Kushnir, M Ting, M Cane, N Naik, J Miller (2007): Would advance knowledge of 1930s SSTs have allowed prediction of the Dust Bowl drought? *Journal of Climate, in press*.

Shindell, D.T., G. Faluvegi, S.E. Bauer, D. Koch, N. Unger, S. Menon, R.L. Miller, G.A. Schmidt, and D.G. Streets, 2007: Climate response to projected changes in short-lived species under the A1B scenario from 2000-2050 in the GISS climate model. *J. Geophys. Res.*, 112, D20103, doi:10.1029/2007JD008753.

Slocum G (1935): Dust Storms, April 1935. *Monthly Weather Review*, **63**, 148

Tegen, I., and I. Fung, 1995:: Contribution to the atmospheric mineral aero-sol load from land surface modification. *J. Geophys. Res.,* **100,** 18 707–18 726.

Vose RS, L Richard, PM Schmoyer, TC Steurer, RH Peterson, KR Thomas, J Eischeid (1992): The Global Historical Climatology Network: long-term monthly temperature, precipitation, sea level pressure, and station pressure data. ORNL/CDIAC-53, NDP-041. Carbon Dioxide Information Analysis Center, Oak Ridge National Laboratory, Oak Ridge, Tennessee.

Worster D (1979): *Dust Bowl: The Southern Plains in the 1930s*. Oxford University Press, New York, 277 pp.

Yoshioka, M., N. Mahowald, J.-L. Dufresne, and C. Luo (2005), Simulation of absorbing aerosol indices for African dust, J. Geophys. Res., 110, D18S17, doi:10.1029/2004JD005276.

Yoshioko M, N Mahowald, AJ Conley, WD Collins, DW Fillmore, CS Zender, DB Coleman (2007): Impact of Desert Dust Radiative Forcing on Sahel Precipitation: Relative Importance of Dust Compared to Sea Surface Temperature Variations, Vegetation Changes, and Greenhouse Gas Warming. *Journal of Climate*, doi:10.1175/JCLI4056.1

343 **Figure Legend**

344 Figure 1. Net dust emissions (Emission-Deposition) for the Dust Bowl source region
345 (34ºN-48ºN, 102.5ºW-92.5ºW), for each member of the SST+Dust ensemble. EJ1, EJ2,
346 etcetera refer to individual ensemble members, each with a unique initial condition.

347

348 Figure 2: Ensemble mean differences in total atmospheric dust loading, g m^{-2},
349 Experiment 3 (SST+Dust) minus Experiment 2 (SST only). Outlined are the eight grid
350 boxes that constitute the new dust source in the SST+Dust experiments.

351

352 Figure 3. Box and whisker plots for precipitation anomalies, averaged over the central
353 United States (30ºN-48ºN, 105ºW-85ºW). Shown are data from the GHCN dataset and
354 output from the three ModelE experiments: SST forcing (1920-1929), SST forcing (1932-
355 1939), and SST+Dust forcing (1932-1939). For GHCN data, anomalies are relative to
356 GHCN data for 1920-1929. For model experiments, anomalies are relative to the SST
357 forcing (1920-1929) experiment. Plots for the GHCN anomalies are based on 10 years
358 (1920-1929) and 8 years (1932-1939); for the model output, each plot represents output
359 from five member ensembles simulations; 50 years for 1920-1929 and 40 years for 1932-
360 1939.

361

362 Figure 4. Spatial extent and magnitude of precipitation anomalies. Anomalies are
363 relative to the same reference period in Figure 3.

364

365

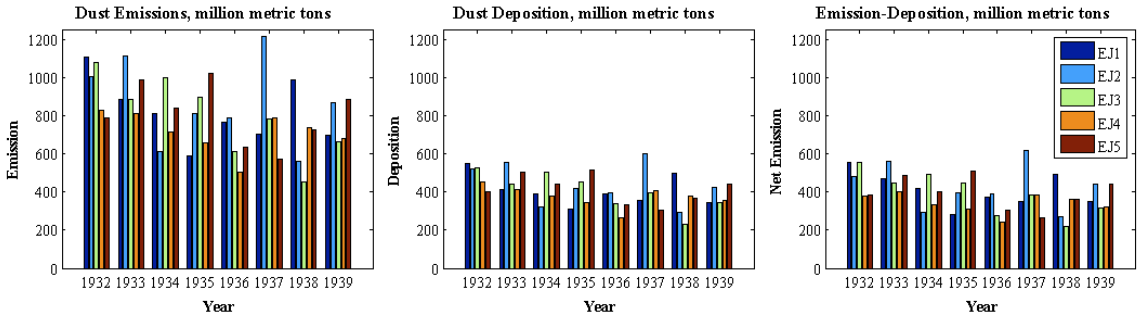

366

367 **Figure 1**

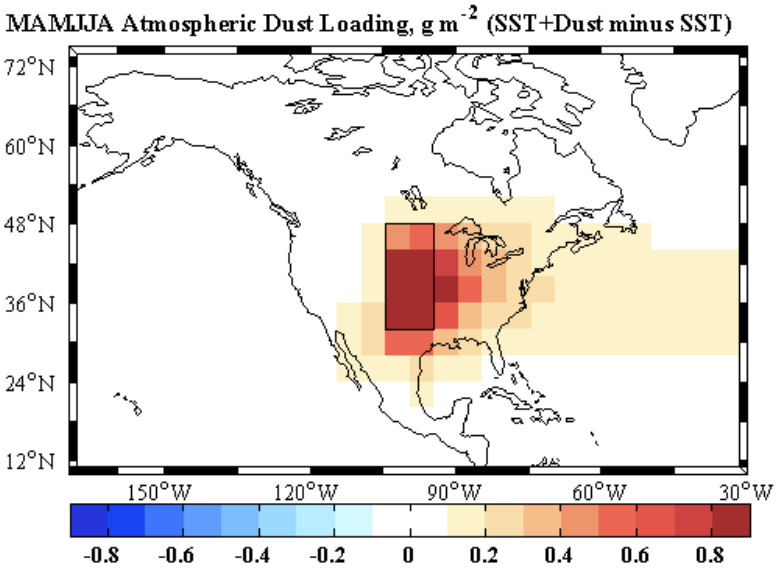

368

369 **Figure 2**

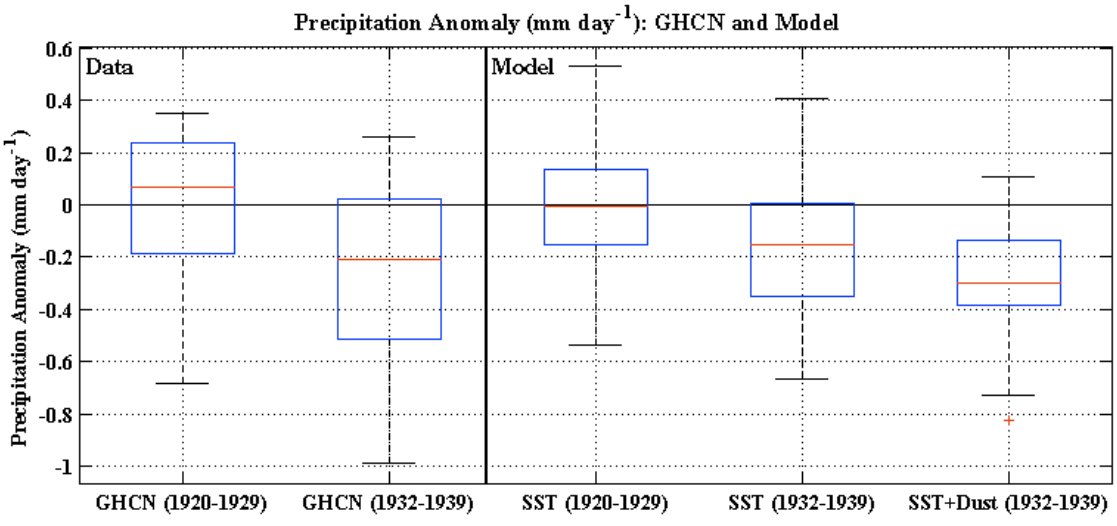

370

371 **Figure 3**

372

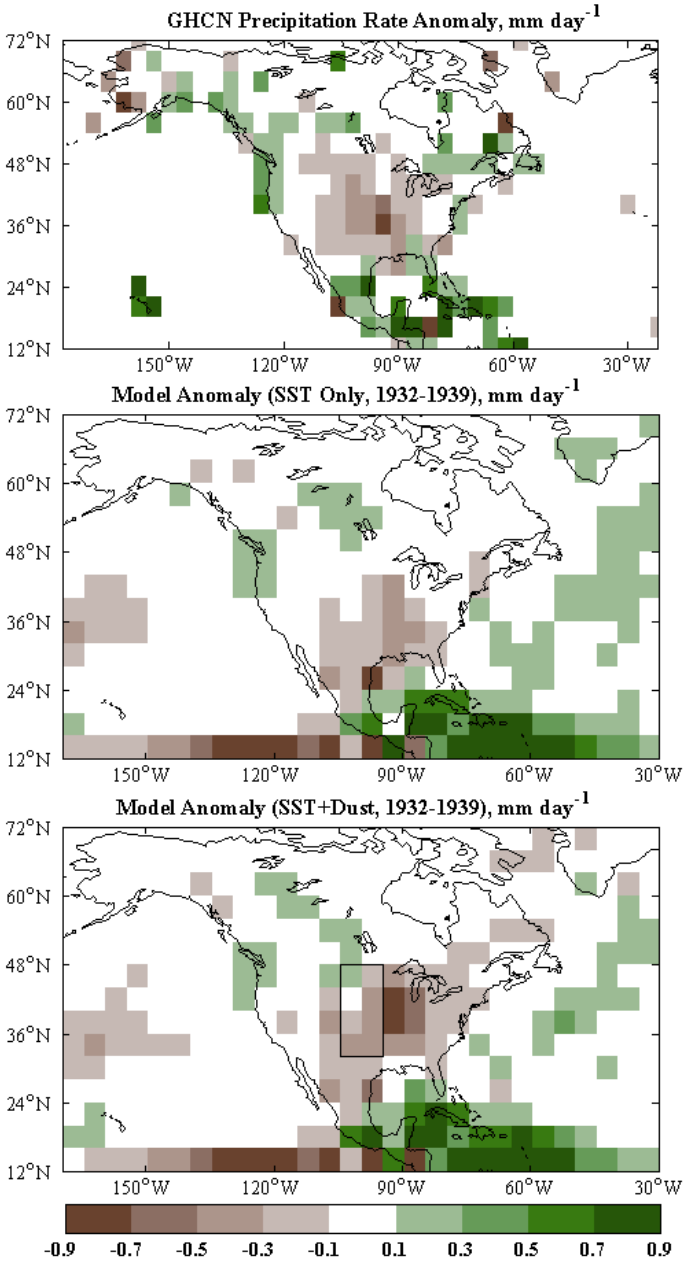

373

374 **Figure 4**